Chiral Xyliphos Complexes for the Catalytic Imine Hydrogenation Leading to the Metolachlor Herbicide: Isolation of Catalyst–Substrate Adducts[+]

Romano Dorta,*[a] Diego Broggini,[b] Robert Stoop,[c] Heinz Rüegger,[c] Felix Spindler,[d] and Antonio Togni[c]

Abstract: Iridium complexes relevant to the catalytic enantioselective hydrogenation of 2-methyl-6-ethylphenyl-1′-methyl-2′-methoxyethylimine (MEA-imine, **1**) in the Syngenta Metolachlor (**3**) process were prepared and characterized. Reaction of the diphosphane (*S*)-1-[(*R*)-2-(diphenylphosphanyl)ferrocenyl]ethyldi(3,5-xylyl)phosphane ((*S*)-(*R*)-Xyliphos, (*S*)-(*R*)-**4**) with $[Ir_2(\mu\text{-}Cl)_2(cod)_2]$ (cod = 1,5-cyclooctadiene) afforded [Ir(Cl)(cod){(*S*)-(*R*)-**4**}] (**7**), which reacted with $AgBF_4$ to form $[Ir(cod)\{(S)\text{-}(R)\text{-}\mathbf{4}\}]BF_4$ (**8**). Complexes **7** and **8** reacted with iodide to yield [Ir(I)(cod){(*S*)-(*R*)-**4**}] (**9**). When **9** was treated with one and two equivalents of HBF_4, two isomers of the cationic Ir^{III} iodo hydrido complex $[Ir(I)(H)(cod)\{(S)\text{-}(R)\text{-}\mathbf{4}\}]BF_4$ were isolated (**10** and **11**, respectively). Complex **9** was oxidized with one equivalent of I_2 to give the iodo-bridged dinuclear species $[Ir_2I_2(\mu\text{-}I)_3\{(S)\text{-}(R)\text{-}\mathbf{4}\}_2)]I$ (**12**). $[Ir_2(\mu\text{-}Cl)_2(coe)_4]$ (coe = cyclooctene) reacted with (*S*)-(*R*)-**4** to yield the chloro-bridged dinuclear complex $[Ir_2(\mu\text{-}Cl)_2\{(S)\text{-}(R)\text{-}\mathbf{4}\}_2]$ (**13**). Complexes **7**–**12** were structurally characterized by single-crystal X-ray diffraction and tested as single-component catalyst precursors for enantioselective hydrogenation of MEA-imine. Complex **10** and dinuclear complex **12** gave the best catalytic results. Efforts were also directed at isolating substrate– or product–catalyst adducts: Treatment of **8** with 2,6-dimethylphenyl-1′-methyl-2′-methoxyethylimine (DMA-imine, **14**, a model for **1**) under H_2 allowed four isomers of $[Ir(H)_2\{(S)\text{-}(R)\text{-}\mathbf{4}\}(\mathbf{14})]BF_4$ (**18**–**21**) to be isolated. These analytically pure isomers were fully characterized by 2D NMR techniques. X-ray structural analysis of an Ir^I–imine adduct, namely, $[Ir(C_2H_4)_2(\mathbf{14})]BF_4$ (**25**), which was prepared by reacting $[IrCl(C_2H_4)_4]$ with $[Ag(\mathbf{14})_2]BF_4$ (**16**), confirmed the κ^2 coordination mode of imine **14**.

Keywords: asymmetric catalysis · hydrogenation · iridium · P ligands

Introduction

Chiral amines constitute an important class of biologically active molecules. Catalytic enantioselective hydrogenation of imines is an efficient method to prepare chiral amines.[1] Iridium is particularily efficient in the catalytic hydrogenation of "difficult" substrates such as tetrasubstituted alkenes[2] and imines.[3–5] The key steps in the industrial syntheses of dextrometorphan (Lonza)[6] and (1*S*)-Metolachlor (Syngenta)[7] are both enantioselective imine hydrogenations catalyzed by soluble chiral iridium ferrocenyldiphosphane complexes. The latter synthesis is outlined in Scheme 1 and features the hydrogenation of 2-methyl-6-ethylphenyl-1′-methyl-2′-methoxyethylimine (MEA-imine, **1**) to the optically enriched (80% *ee*) (*S*)-MEA-amine (**2**). Nowadays, this reaction represents the largest scale enantioselective catalytic process in industry. Compound **2** is the precursor to the chiral herbicide (1*S*)-Metolachlor (**3**)[8,9] which is sold under the trademark Dual-Magnum in amounts of more than 10 000 t per annum.[10]

The industrial catalyst system is prepared in situ and consists of a mixture of $[Ir_2(\mu\text{-}Cl)_2(cod)_2]$ (cod = 1,5-cyclooctadiene), the chiral diphosphane (*R*)-(*S*)-Xyliphos ((*R*)-1-[(*S*)-2-(diphenylphosphanyl)ferrocenyl]ethyldi(3,5-xylyl)phosphane, (*R*)-(*S*)-**4**), iodide (as tetrabutylammonium or sodium salt), and a Brønsted acid (e.g., acetic or sulfuric acid). The reaction is carried out under 80 bar of hydrogen

[a] Prof. Dr. R. Dorta
Departamento de Química
Universidad Simón Bolívar,
Caracas 1080A (Venezuela)
Fax: (+58) 212-9063961
E-mail: rdorta@usb.ve

[b] Dr. D. Broggini
Department of Chemistry and Biochemistry, University of California
Santa Barbara, CA 93106-9510 (USA)

[c] Dipl. Chem. R. Stoop, Dr. H. Rüegger, Prof. Dr. A. Togni
Laboratory of Inorganic Chemistry,
Swiss Federal Institute of Technology
ETH Hönggerberg, 8093 Zürich (Switzerland)

[d] Dr. F. Spindler
Solvias AG, Postfach, CH-4002 Basel (Switzerland).

[+] The major part of this work was carried out by R.D. at ETH (ETH Diss. No. 12739).

 DOI: 10.1002/chem.200305218

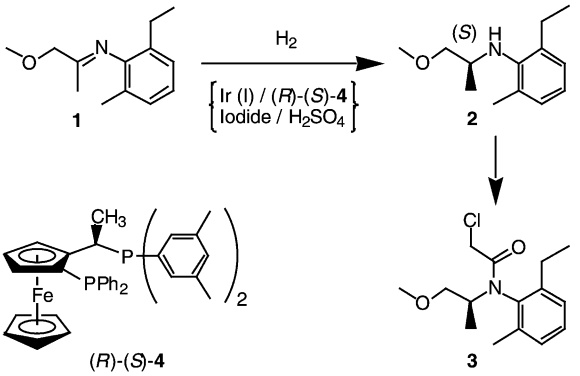

Scheme 1. Industrial synthesis of Metolachlor (Syngenta).

pressure at 323 K with a substrate/catalyst ratio of 10^6. Initial turnover frequency (TOF) is said to exceed $1.8\times 10^6\ h^{-1}$.[10] This makes it one of the fastest homogeneous systems known, second only to certain homogeneous Ziegler–Natta polymerization catalysts[11] and Noyori's ruthenium hydrogenation catalysts.[12] Here we present the synthesis and characterization (including X-ray crystal structures) of iridium complexes that reflect the composition of the "magic mixture" that is used in industry to hydrogenate MEA-imine. These complexes were tested as single-component catalyst precursors in the MEA-imine hydrogenation. The best catalytic results were obtained with an iodo-bridged Ir^{III} dimer which was synthesized by oxidation of an Ir^{I} precursor with I_2. Furthermore, we present the isolation and full characterization of catalyst–substrate adducts and an X-ray analysis of a related iridium imine complex.

Results and Discussion

Ligand synthesis: The secondary phosphane $(3,5\text{-Xyl})_2PH$ (**5**) was obtained from $PCl_2(NEt_2)$ in three steps in 59% yield (Scheme 2). Condensation of **5** with commercially available (*S*)-*N*,*N*-dimethyl-1-[(*R*)-2-(diphenylphosphanyl)-ferrocenyl]ethylamine (**6**)[13] was accomplished by following the standard protocol[14] and gave 75% of yellow microcrystalline (*S*)-(*R*)-**4**. The $^{31}P\{^1H\}$ NMR spectrum showed a pair of doublets at $\delta=-25.2$ and 6.5 ppm ($J=19$ Hz). Note that this is the enantiomer of the ligand that is used in the technical application, but this does not affect the scope of this work.

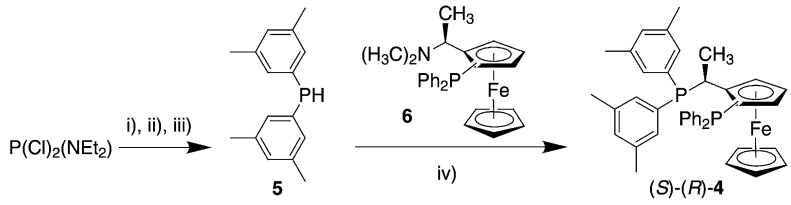

Scheme 2. Synthesis of (*S*)-(*R*)-**4**. i) 2 equiv 3,5-Xyl-Li, 203 K, Et_2O; ii) 4 equiv, HCl(g), Et_2O; iii) LAH, 195 K, Et_2O; iv) AcOH, 370 K.

Syntheses of complexes: The "magic" catalyst mixture used in industry to hydrogenate **1** consists of $[Ir_2(\mu\text{-}Cl)_2(cod)_2]$, two equivalents of diphosphane **4**, Bu_4NI or NaI, and H_2SO_4 or AcOH. We expected that once the neutral Ir^{I} diphosphane complex bearing either Cl^- or I^- ligands is formed in situ it will readily be protonated to form cationic Ir^{III} hydrido species. In fact, we observed the formation of several iridium diphosphane hydride species when all four aforementioned ingredients were mixed under one-pot reaction conditions. Unfortunately, no procedure was found to separate the different components of these mixtures. We therefore decided to synthesize such complexes in a step-by-step manner and to test them subsequently as one-component catalyst precursors for the hydrogenation of **1**.

$[Ir_2(\mu\text{-}Cl)_2(cod)_2]$ reacted cleanly with two equivalents of (*S*)-(*R*)-**4** in toluene to afford [Ir(Cl)(cod){(*S*)-(*R*)-**4**}] (**7**) in good yield as a yellow powder. The $^{31}P\{^1H\}$ NMR spectrum indicated the formation of a sole diastereomer by the presence of only one pair of doublets ($J=37$ Hz) at $\delta=16.4$ and -14.5 ppm. Complex **7** was treated with one equivalent of $AgBF_4$ in THF to afford the cationic compound **8** [see Eq. (1)] as a brick-red powder in excellent yield. All ^{31}P, ^{13}C, and ^1H resonances were assigned by standard 2D NMR techniques (see Experimental Section). A pair of doublets ($J=24$ Hz) at $\delta=3.2$ ($P(Ph)_2$) and at 37.9 ppm ($P(Xyl)_2$) in the $^{31}P\{^1H\}$ NMR spectrum characterized **8**. In the ^{13}C NMR spectrum the C atoms of the coordinated olefins *trans* to the xylyl- and phenyl-substituted P atoms resonated at $\delta=92.3$, 86.0 and 91.2, 84.7 ppm, respectively. This indicates that electronically these latter donors are only modestly different, the xylyl-substituted one exerting a slightly larger *trans* influence. The electronic imbalance between the two ends of each double bond is mainly a consequence of the twisted conformation that the cod ligand adopts to fit into the chiral pocket generated by the aryl groups of the Xyliphos ligand (see X-ray structure analysis below). All observations were in accord with results for analogous complexes characterized by a number of selective NOEs and homo- and heteronuclear coupling constants[15] and by single-crystal X-ray diffraction study (see Figure 1). We reasoned that the co-catalysts $[N(Bu)_4]I$ and H_2SO_4 used in the industrial system can form HI in situ. Therefore, we studied the reactivity of **8** toward commercially available aqueous HI under different conditions, and we invariably observed the formation of a mixture of mainly two hydride species. The ^1H NMR spectra of the resulting solutions showed a doublet of doublets at $\delta=-13.8$ ppm and a pseudotriplet at $\delta=-12.6$ ppm in varying ratios, along with signals for small amounts of other hydrides. Disappointingly, these reactions were neither clean nor could the products be separated. A stepwise synthesis in which **8** was first treated with iodide and then protonated proved to be more successful. Thus, the Ir^{I} iodide **9** was prepared from **8** by adding one equivalent

of $[N(Bu)_4]I$ in THF [Eq. (1)]. Alternatively, halogen exchange of **7** with one equivalent of KI in acetone directly led to **9**, which was isolated as a yellow powder. Remarkably, both routes to **9** involved absolute (at the NMR-sensitivity level) diastereoselectity of the I^- addition. Single-crystal X-ray diffraction on **9** revealed that the Ir–I bond is oriented *endo* with respect to the ferrocene moiety (see Figure 2). Compounds **7**, **8**, and **9** were easily prepared on gram scales.

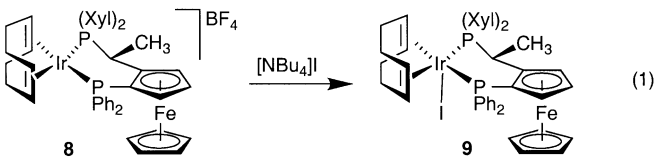

(1)

Single crystals of **8** suitable for an X-ray diffraction study were grown from THF. Figure 1 shows the expected square-planar coordination environment of iridium. The iridium

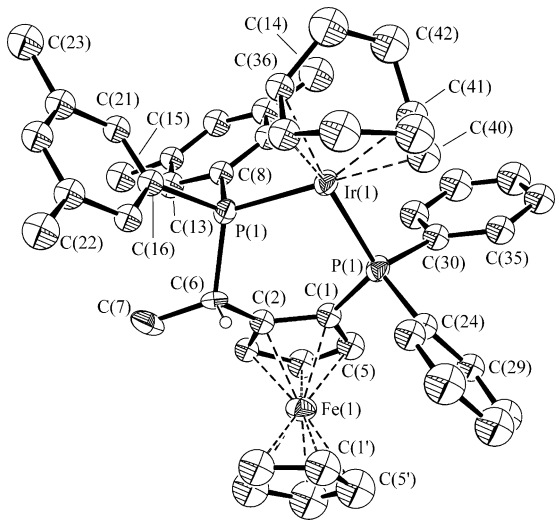

Figure 1. Structure of the cation of **8** (ORTEP plot; 30% probability ellipsoids). Selected bond lengths [Å] and angles [°]: Ir(1)–P(1) 2.318(4), Ir(1)–P(2) 2.325(4), Ir(1)–C(36) 2.243(15), Ir(1)–C(40) 2.221(18), Ir(1)–C(37) 2.183(13), Ir(1)–C(41) 2.180(18), C(36)–C(37) 1.37(3), C(40)–C(41) 1.35(2); P(1)-Ir(1)-P(2) 92.76(15), P(1)-Ir(1)-C(40) 89.1(5), P(1)-Ir(1)-C(41) 94.8(5), P(2)-Ir(1)-C(36) 89.4(4), P(2)-Ir(1)-C(37) 95.2(5).

atom lies within 0.02 Å of the best plane fitted through P(1), P(2), and the midpoints of the C=C bonds. The cod ligand is appreciably twisted out of the P(1)-Ir(1)-P(2) plane. This is best illustrated by the distances of C(37) and C(41) from this plane of −1.05 and +1.12 Å, respectively, or, alternatively, by the closeness of C(36) and C(40) to this plane (0.26 and −0.17 Å, respectively). Thus, the solid-state structure is in accord with the electronic imbalance of the two double bonds of the cod ligand that was observed in NMR experiments.

Single crystals of **9** were obtained from a THF/Et_2O mixture. Complex **9** crystallized in a very large unit cell that contains four molecules. There are two crystallographically distinct molecules. Figure 2 shows the square-pyramidal coordination environment of one of the two independent mol-

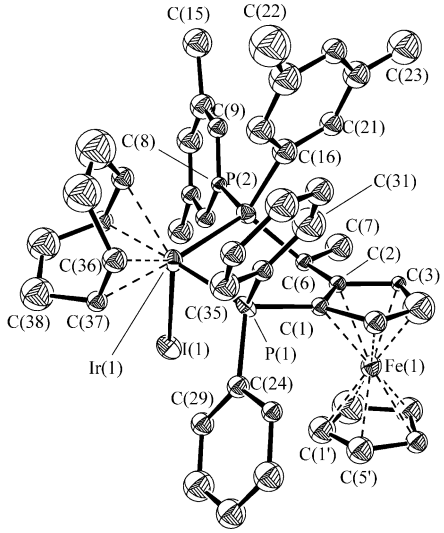

Figure 2. Structure of one of the two independent molecules of **9** (ORTEP plot; 30% thermal isotropic ellipsoids). Selected bond lengths [Å] and angles [°]: Ir(1)–I(1) 2.888(4), Ir(1)–P(1) 2.357(12), Ir(1)–P(2) 2.353(13), Ir(1)–C(36) 2.15(5), Ir(1)–C(37) 2.16(5), Ir(1)–C(40) 2.19(4), Ir(1)–C(41) 2.23(5), C(36)–C(37) 1.25(6), C(40)–C(41) 1.40(6); I(1)-Ir(1)-P(1) 97.2(3), I(1)-Ir(1)-P(2) 90.6(3), P(1)-Ir(1)-P(2) 98.9(5), I(1)-Ir(1)-C(36) 122.9(14), P(1)-Ir(1)-C(36) 86.5(15), I(1)-Ir(1)-C(41) 120.9(12), P(2)-Ir(1)-C(41) 86.5(15), I(1)-Ir(1)-C(40) 85.1(12).

ecules of **9**. The iodine atom is oriented in the direction of the ferrocenyl moiety, which is a recurring feature in ferrocenyl diphosphane iridium complexes[16,17] (vide infra). The iridium atom is displaced 0.37 Å along the Ir(1)–I(1) vector out of the best plane fitted through P(1), P(2), and the midpoints of the C=C bonds of the cod ligand. The Ir(1)–I(1) distance of 2.888(4) Å is significantly longer than in the corresponding Ir^{III} species (vide infra). The double bond C(36)=C(37) (1.25(6) Å) *trans* to the more basic phosphane P atom P(2) is shorter than C(40)=C(41) (1.40(6) Å). However, the large standard deviations of the bond lengths preclude a more detailed discussion of the bonding parameters. We note that no significant difference in the *trans* influence of the phosphanes in the X-ray structure of the corresponding cationic complex **8** was detected.

The well-characterized, diastereomerically pure, neutral iodo complex **9** was then used in protonation studies. Reaction of **9** with H_2SO_4, CH_3COOH, and CF_3SO_3H in different solvents invariably led to mixtures of hydrides. However, slow addition of a solution of HBF_4 in Et_2O to a solution of **9** in CH_2Cl_2 at 195 K afforded one hydrido species in 90% yield, based on NMR measurements. The pseudotriplet at $\delta = -12.6$ ppm in the ^1H NMR spectrum corresponded to a pair of doublets ($J = 18$ Hz) at $\delta = -12.4$ and 23.5 ppm in the $^{31}P\{^1H\}$ NMR spectrum. After workup, **10** (Scheme 3) was isolated as a pink powder and fully characterized. Its structure is in accordance with standard 2D NMR data. Treatment of **9** with two equivalents of HBF_4 or, alternatively, of

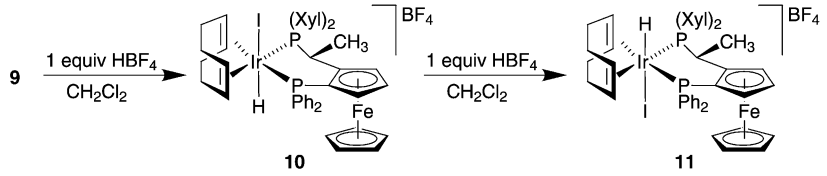

Scheme 3. Synthesis of **10** and **11**.

10 with a further equivalent of HBF_4 gave a new iridium hydride complex which was isolated in acceptable yields as an orange powder. This compound was characterized by a doublet of doublets ($J_1 = 15.8$, $J_2 = 9.3$ Hz) at $\delta = -13.8$ ppm in the hydrido region of the ^{1}H NMR spectrum and by a pair of doublets ($J = 23$ Hz) at $\delta = -31.9$ and -1.5 ppm in the ^{31}P{^{1}H} NMR spectrum. Full characterization, including a single-crystal X-ray diffraction analysis (see Figure 3), allowed us to formulate the product as **11** (Scheme 3). The protonation mechanism has not yet been elucidated and is far from clear.[18] However, most important for the scope of this study is the fact that we succeeded in isolating and characterizing two monomeric iridium hydrido iodo isomers in pure form that are the formal oxidative addition products of HI to **8**. These two isomers, **10** and **11**, were also present in the above mentioned "magic mixture" when typical precatalyst preparation protocols were followed. Indeed, both **10** and **11** were excellent precatalysts for the hydrogenation of MEA-imine **1** (vide infra).

Single crystals of **11** suitable for an X-ray study were grown from a THF/CH_2Cl_2 mixture. Figure 3 shows a pseudooctahedral coordination environment of iridium, with the axial iodide ligand pointing in the direction of the ferrocenyl moiety. The Ir(1)–I(1) bond length of 2.803(5) Å compares well with that of one of the rare structurally characterized mononuclear iridium iodo hydrides.[19] Figure 4 is a superposition of the core structures of **9** and **11**. The presence of the hydride ligand in **11** forces the cod ligand to twist by 15° into the equatorial plane relative to its orientation in **9**. Alternatively, this situation may be described by the smaller distance of the iridium atom from the best plane fitted through P(1), P(2), and the midpoints of the C=C bonds of cod in **11**, that is, 0.23 in **11** versus 0.37 Å in **9**.

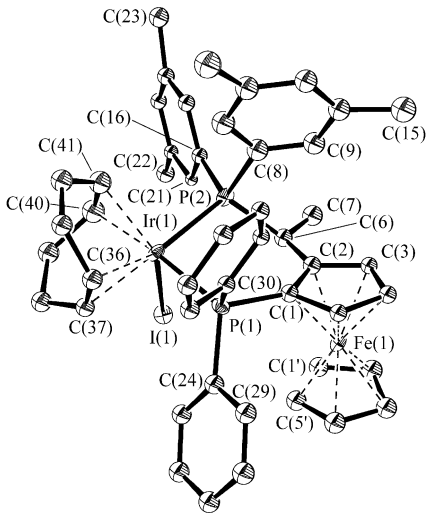

Figure 3. Structure of the cation of **11** (ORTEP plot; 30% probability ellipsoids). Selected bond lengths [Å] and angles [°]: Ir(1)–I(1) 2.803(5), Ir(1)–P(1) 2.357(16), Ir(1)–P(2) 2.349(16), Ir(1)–C(36) 2.22(4), Ir(1)–C(37) 2.22(4), Ir(1)–C(40) 2.28(4), Ir(1)–C(41) 2.22(4), C(36)–C(37) 1.26(8), C(40)–C(41) 1.28(8); P(1)-Ir(1)-P(2) 90.9(5), I(1)-Ir(1)-P(1) 94.9(4), I(1)-Ir(1)-P(2) 90.4(4), C(36)-Ir(1)-I(1) 116.3(16), C(37)-Ir(1)-I(1) 83.7(16), C(41)-Ir(1)-I(1) 113.5(18), C(40)-Ir(1)-I(1) 80.9(17), C(36)-Ir(1)-P(2) 153.4(16), C(36)-Ir(1)-P(2) 153.4(16), C(41)-Ir(1)-P(2) 88.0(18), C(40)-Ir(1)-P(2) 92.8(18), C(36)-Ir(1)-P(1) 86.6(16), C(37)-Ir(1)-P(1) 94.5(17), C(41)-Ir(1)-P(1) 151.5(18), C(40)-Ir(1)-P(1) 174.5(17).

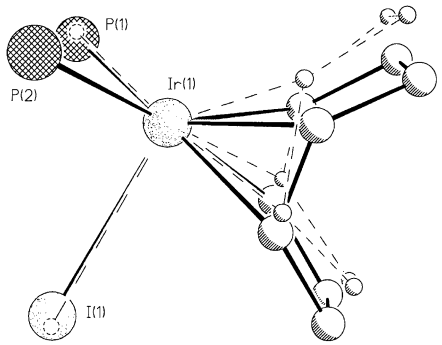

Figure 4. Superposition of the coordination environments of iridium in complexes **9** and **11**.

The attempted oxidative addition of I_2 to **8** led to an unprecedented enantioselective activation and subsequent iodination of an allylic C–H bond of the coordinated cod ligand with concomitant formation of an Ir^{III} hydrido iodo cation. This chemistry has been described in detail elsewhere.[17] When complex **9** was treated with an equimolar amount of I_2 in toluene at 333 K, a new species formed quantitatively according to NMR spectroscopy [Eq. (2)]. The ^{1}H NMR spectrum revealed the absence of coordinated cod and coordinated solvent molecules. Elemental analyses were in agreement with a compound of the composition Ir·I_3·**4**. Molecular weight determination indicated a dinuclear structure. Conductometric measurements in acetone were in agreement with a 1:1 electrolyte. The ^{31}P{^{1}H} NMR spectrum showed a sharp pair of doublets ($J = 11$ Hz) at $\delta = -22.0$ and 2.0 ppm and thus suggested a C_2-symmetric dinuclear complex. Finally, a single-crystal X-ray analysis (see Figure 5) was in agreement with these findings and allowed us to draw structure **12**. This complex reacted neither with Tl and Ag salts nor with strong Brønsted acids. Nonetheless, **12** turned out to be the most efficient single-component catalyst for MEA-imine hydrogenation (vide infra).

Crystals of **12** suitable for an X-ray crystallographic analysis were grown from a CH_2Cl_2/Et_2O mixture. In view of the large dimensions of the structure the *R* values are high, and the accuracy of the bonding parameters is correspondingly low (in fact, no meaningful esd values were calculated). Figure 5 confirms the dinuclear monocationic nature of **12**

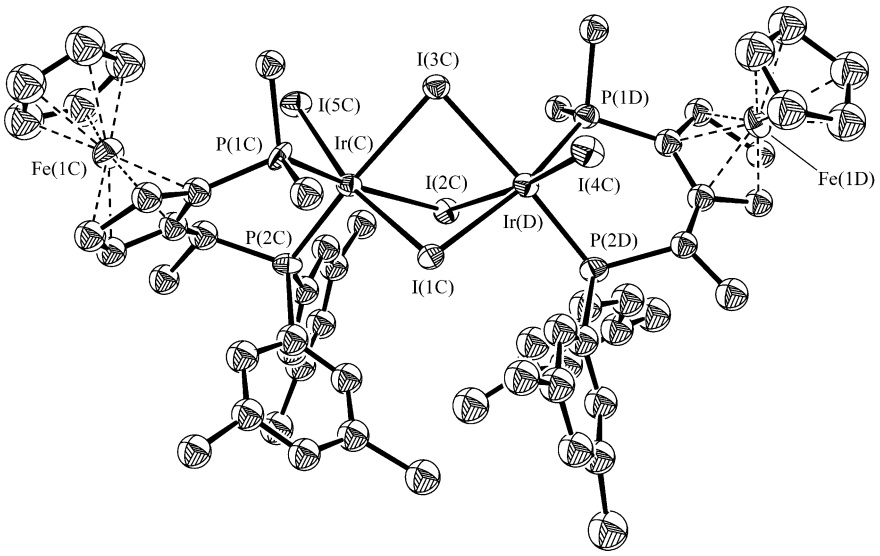

Figure 5. Structure of one of the two independent cations of **12** (ORTEP plot; 30% probability ellipsoids). For clarity only the *ipso*-C atoms of the phenyl groups are drawn. Selected bond lengths [Å] and angles [°]: Ir(C)–Ir(D) 3.669, Ir(C)–I(1C) 2.671(4), Ir(C)–I(2C) 2.770(4), Ir(C)–I(3C) 2.776(4), Ir(C)–I(5C) 2.721(4), Ir(C)–P(1C) 2.249(15), Ir(C)–P(2C) 2.263(15), Ir(D)–I(1C) 2.720(4), Ir(D)–I(2C) 2.697(4), Ir(D)–I(3C) 2.758(4), Ir(D)–I(4C) 2.693(4), Ir(D)–P(1D) 2.356(15), Ir(D)–P(2D) 2.278(16); P(1C)-Ir(C)-I(1C) 95.7(4), P(1C)-Ir(C)-I(3C) 91.6(4), P(1C)-Ir(C)-I(5C) 93.4(4), P(1C)-Ir(C)-P(2C) 95.5(6), P(2C)-Ir(C)-I(1C) 98.8(4), P(2C)-Ir(C)-I(2C) 93.7(4), P(2C)-Ir(C)-I(5C) 90.2(4), I(1C)-Ir(C)-I(2C) 77.62(12), I(1C)-Ir(C)-I(3C) 81.71(13), I(2C)-Ir(C)-I(3C) 79.40(12), I(2C)-Ir(C)-I(5C) 91.86(13), I(3C)-Ir(C)-I(5C) 88.13(13), Ir(C)-I(1C)-Ir(D) 85.76(12), Ir(C)-I(2C)-Ir(D) 84.30(12), Ir(C)-I(3C)-Ir(D) 83.07(12).

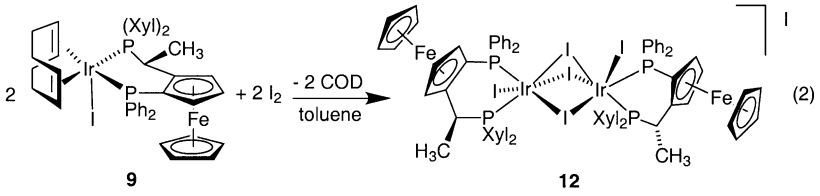

9 **12**

and gives a selection of bond parameters. The triple iodo bridge, along with the two terminal iodides and the two diphosphane ligands, define the two octahedral coordination environments of Ir(1C) and Ir(1D). The terminal iodides I(1C) and I(1D) again point in the direction of the ferrocenyl moieties. Their distances to the iridium centers of about 2.7 Å compare well with other Ir^{III}–I bond lengths[19,21,22] and are shorter than the corresponding distances in the Ir^{I} and Ir^{III} complexes **9** and **11** (vide supra). The Ir–I bonds *trans* to the P atoms are slightly longer than those *trans* to the I atoms. Figure 6 is a view along the molecular C_2 axis that passes through I(3C), and thus shows agreement with solution ^{31}P NMR data (pair of doublets). Structually, **12** appears to be a diphosphane analogue of the nonahalogenoiridates $[Ir_2X_9]^{3-}$[20] in which four of the terminal X^- ligands correspond to the two diphosphane ligands in **12**.

We found that $[Ir_2(\mu\text{-}Cl)_2(coe)_4]$ (coe = cyclooctene) reacted cleanly with diphosphane (*S*)-(*R*)-**4** in benzene, toluene, or THF to give mixtures of the chloro-bridged dinuclear complexes *cis*- and *trans*-**13** in good yields. The ^{31}P NMR spectrum showed two pairs of multiplets, as expected for two AA′BB′ systems. One pair of multiplets is at $\delta = -4.2$ and 22.7 ppm (only $^2J_{PP'} + {}^4J_{PP'} = 38$ Hz was resolved), and the other at $\delta = -1.0$ and 26.7 ppm ($^2J_{PP'} + {}^4J_{PP'} = 31$ Hz). The *cis/trans* ratio (ca. 30/70) appeared to be independent of the reaction conditions (different solvents, temperatures, and ways of mixing $[Ir_2(\mu\text{-}Cl)_2(coe)_4]$ with **4**). Complex **13** is air-sensitive (sometimes pyrophoric), and it did not react with iodides (e.g., Bu_4NI). We recently discovered that olefin-free Ir^{I} dimers such as **13** readily and reversibly react with C–H and O–H bonds,[16] and their catalytic potential was demonstrated in enantioselective olefin hydroamination (via N–H activation)[23] and olefin hydroarylation (via C–H activation)[24] reactions.

Catalytic hydrogenation of MEA-imine (1): Complexes **7**–**12** were tested as catalyst precursors for the enantioselective, solvent-free hydrogenation of MEA-imine (**1**) to MEA-amine (**2**) (Table 1). Unfortunately, the pronounced sensitivity of **13** to air and moisture precluded its use under the experimental conditions chosen here.

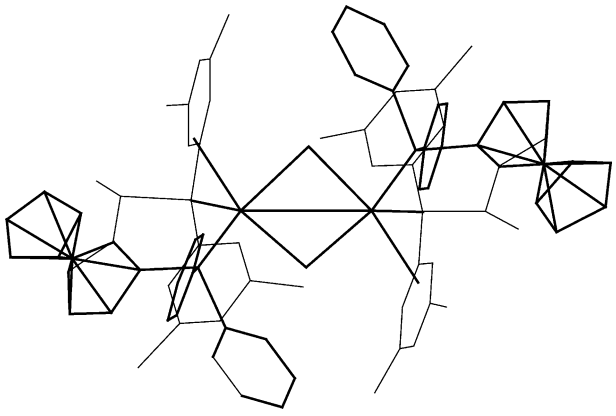

Figure 6. View along the molecular C_2 axis of **12** passing through I(3C) (PowerMoMo line drawing).

Enantioselectivities did not vary significantly with the different precatalysts, but the activities were a function of the Cl, I, or H ligands and the oxidation state of the precatalysts. Notably, the halide-free compound **8** was a very poor hydrogenation catalyst (Table 1, entry 3). The influence of the chloride versus the iodide ligand is evident in entries 2

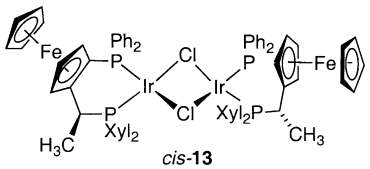

cis-**13**

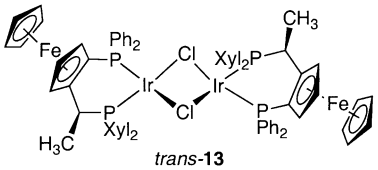

trans-**13**

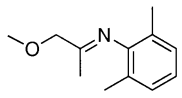

14

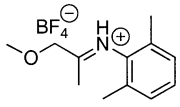

15

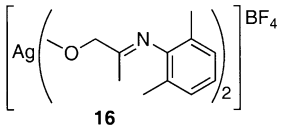

16

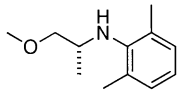

(*R*)-**17**

Table 1. Iridium-catalyzed hydrogenation of **1**[a]

Entry	Catalyst precursor	Yield [%]	TOF [h^{-1}]	ee [%] (config.)
1	reference system[b]	100	2778	80 (*R*)
2	**7**	31.2	867	77 (*R*)
3	**8**	<1	<28	not determined
4	**9**	23.6	656	78 (*R*)
5	**10**	70.0	1944	77 (*R*)
6[c]	**11**	66.0	1375	81 (*R*)
7[d]	**12**	75.0	2083	79 (*S*)

[a] 20.5 mL **1**, no solvent, substrate/catalyst = 50000, $p = 100$ bar, 303 K, 18 h reaction time. See Experimental Section for a typical protocol and analytical methods. [b] $[Ir_2(\mu\text{-}Cl)_2(cod)_2]$ + 2(*S*)-(*R*)-**4** + $[Bu_4N]I$ + AcOH. [c] 24 h reaction time. [d] Precatalyst of opposite chirality, that is, bearing ligand (*R*)-(*S*)-**4**.

and 4, whereby the latter ligand had a slightly detrimental effect on activity. The Ir^I complexes performed poorly, while the trivalent iridium precatalysts **10**–**12** displayed markedly higher activities. The best mononuclear single-component precatalyst was the cationic iodo hydrido species **10** (Table 1, entry 5), whereas its isomer **11** was less active (Table 1, entry 6). Surprisingly, the dinuclear Ir^{III} precatalyst **12** gave the best results in terms of activity, and selectivity even in the absence of a source of protons (Table 1, entry 7). In fact, under the hydrogenation conditions used in this study, iridium hydrido iodo species may be formed along with HI. Likewise, Zhang et al. recently used iodine as an efficient in situ co-catalyst in the iridium-catalyzed enantioselective hydrogenation of arylimines. They proposed heterolytic H_2 activation by an $Ir(\widehat{PP})(Cl)(I)_2$ species to form an iridium hydrido chloro iodo complex with HI elimination.[5] It remains to be demonstrated, though, that HI elimination is favored over HCl elimination. None of the single-component catalysts tested here approached the exceptional activity of the reference system (Table 1, entry 1).[25] These results seem to indicate that both halide ligands, Cl^- as well as I^-, must be present in the reaction mixture.

Isolation and characterization of catalyst–substrate complexes: We were interested in isolating and characterizing complexes that could serve as model compounds for intermediates in the catalytic MEA-imine hydrogenation cycle.[3] We chose to use the slightly simpler model substrate DMA-imine (**14**). Iridium complexes containing both ligand **4** and imine **14** within their coordination spheres are of particular interest since they allow the interplay of steric and electronic factors between the ligand and the substrate to be assessed. In its free state at room temperature imine **14** exists as a mixture of *E* and *Z* isomers in a ratio of 86:14. Complexes **7** and **8** reacted neither with **14** nor with its immonium tetrafluoroborate salt **15**. Complex **9** was protonated by **15** to give a mixture of the hydrido complexes **10** and **11** (along with other minor hydrides) and free imine **14**. Elimination of HI from **10** and **11** took place in part in the presence of **14** (and other bases) to give cationic **8**. Complex **12** did not react with **14**–**16**. The chloro bridge of **13** was not split even in neat imine **14**, nor was any other type of imine coordination observed in NMR experiments. However, as expected, **13** activated the N–H bond of the immonium salt **15** to give complicated and inseparable mixtures of hydrido imino complexes. Treating **13** with silver salt **16** invariably formed complex mixtures and a silver mirror on the walls of the reaction flask.

When the cationic complex **8** was treated with H_2 in the presence of a large excess of DMA-imine (**14**) in CH_2Cl_2, imine adducts **18**–**21** formed [Eq. (3)]. These compounds were isolated as an analytically pure mixture in a ratio of **18**:**19**:**20**:**21** of 45:42:3:10. The diastereoselectivity of this reaction varied little with the reaction conditions employed, such as solvent and temperature. Reactions in CH_2Cl_2 were cleaner than in CH_3OH, THF, or neat **14**. At 195 K, the reaction was considerably slower, but with no beneficial effect on the diastereoselectivity of DMA-imine complexation. Although separation of isomers **18**–**21** was not possible, their solution structures were fully established by a combination of multinuclear 1D and 2D NMR techniques. The κ^2 coordination mode of imine **14** in another iridium complex was confirmed by an X-ray structure analysis (**25**, vide infra). Characteristic NMR parameters are summarized in Table 2. A phase-sensitive $^{31}P,^1H$ COSY experiment 1) established the type of substituents on the phosphorus donors, 2) assigned the resonances of the hydride ligands *trans* to P from the magnitudes of the $J(^{31}P,^1H)$ coupling constants, and 3) identified the second hydride ligand. The stereochemistry of this hydride followed from a short triangulation based on cross-peaks observed in the ^1H NOESY experiment. Therefore, in the two major isomers **18** and **19** short internuclear

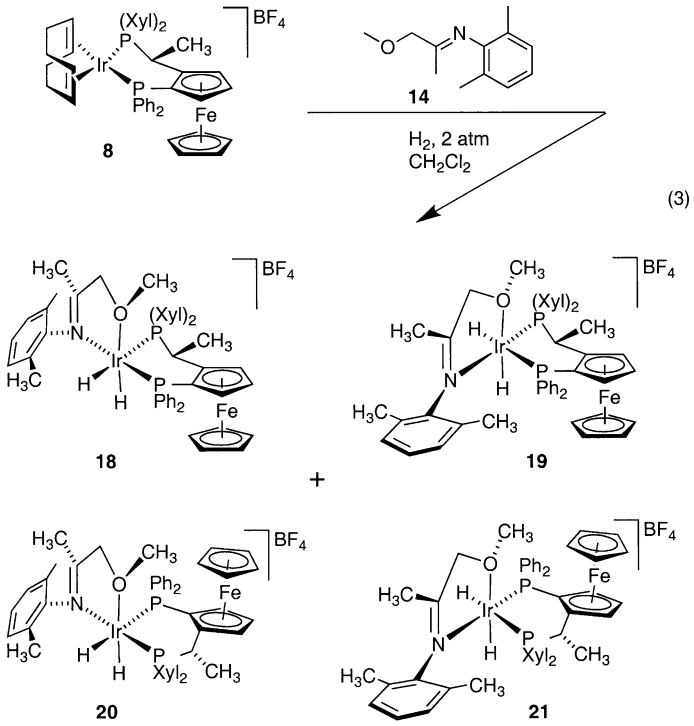

Table 2. Selected NMR data for **18**–**21** (relative abundances).

	18 (45%)	**19** (42%)	**20** (3%)	**21** (10%)
$\delta(^{31}P)$ (PPh_2)	−4.4	−30.2	5.4	−1.0
$\delta(^{31}P)$ ($PXyl_2$)	22.3	11.9	30.8	42.1
$\delta(^1H)$ (J_{trans}, J_{cis})	−6.95 (147, 21.5)	−6.14 (149.9, 19.3)	−7.35 (145.2, 22.7)	−8–06 (153.5, 20.0)
$\delta(^1H)$ (J_{cis}, J_{cis})	−29.86 (13.2, 24.7)	−30.19 (12.6, 25.6)	−30.63 (13.9, 21.8)	−31.69 (8.5, 28.1)
$\delta(^1H)$ (OCH_3)	1.39	1.72	not observed	2.18
$\delta(^1H)$ (OCH_2)	4.48, 4.02	4.47, 4.20	not observed	3.94, 3.07
$\delta(^1H)$ (CH_3)	1.60	1.67	not observed	1.41
$\delta(^1H)$ (C_5H_5)	3.50	3.45	3.58	3.46

separations of these hydrides from 1) the methine protons at the stereogenic center of the phosphorus chelate, 2) the unsubstituted Cp ring, and 3) two types of aromatic *ortho* protons were found. In diastereomers **20** and **21** only the last-named type of interactions was observed, consistent with the remoteness of these hydrides from the aforementioned functional groups. Coordination of the imine ligand in **18** and **19** was proven by the presence of a phosphorus-induced doublet of doublets in the ^{13}C NMR spectrum of the imine C atoms resonating at $\delta = 180.00$ and 180.64 ppm, respectively. Furthermore, the chiral environment around iridium rendered the methylene protons of the coordinated imine diastereotopic. These were individually assigned in **18**, **19**, and **21** from selective NOEs to the *trans-cis* hydride (relative to the P donors) and to the characteristic *ortho* protons of the respective aromatic moieties. The observed selectivity also pointed to a coordination of the ether functionality, as free rotation of the $-CH_2OCH_3$ group is expected to lead to a series of nonselective distance-dependent interactions. The proposed coordination through oxygen is independently supported by the remarkable chemical shifts of the methoxy groups resonating at $\delta = 1.39$, 1.72, and 2.18 ppm for **18**, **19**, and **21**, respectively. These fairly low values for methoxy groups are caused by the shielding anisotropy of the perpendicular aromatic rings which sandwich the methoxy group. The orientation of the imine ligand with respect to the IrH_2P_2 core was established following two short triangulations based on the short internuclear distances that were observed in the NOESY spectrum. The hydrides located *cis* to both P donors exhibited spatial closeness to one of the methyl groups of the 2,6-dimethylaniline unit, whereas *ortho* protons of aromatic moieties assigned to the other hemisphere with respect to the mentioned hydrides are close to the methoxy groups.

A chemically relevant conformational aspect of the diastereomeric mixture **18**–**21** is its solution dynamics. In the room-temperature NOESY spectrum with an exchange mixing time of 600 ms, selective exchange between diastereomers **18** and **21** was observed. An exchange mechanism must be consistent with the observation that the hydride originally *trans* to $PXyl_2$ must end up in the *cis-cis* position (with respect to $\widehat{PP}$) while the other becomes *trans* to $PXyl_2$. Therefore, we suggest dissociation of the ether group, movement of the $PXyl_2$ donor to this vacant position and recoordination of the ether group in the position where $PXyl_2$ left. Although we did not observe further interconversions among the diastereomers it is conceivable that they occur at somewhat slower rates and would explain why constant diastereomer ratios were observed and why the mixtures were inseparable.

Note that migratory insertion of the C=N bonds into the Ir–H bonds of **18** and **20** on the one hand, and of **19** and **21** on the other hand would give rise to amines (*R*)-**17** and (*S*)-**17**, respectively. However, under these conditions (i.e., in absence of halides and at low H_2 pressure) no reaction took place. Although pre-coordination of the imine appears not to be the enantioselective step, structures **18**–**21** allow for some important stereochemical observations:

1) The relative abundances of the diastereomers indicate that the half of the iridium coordination octahedron into which the FeCp moiety points is sterically less accessible for the substrate molecule. In all crystal structures of octahedral or square-pyramidal iridium ferrocenyldiphosphane complexes this position is occupied by a halogen atom.[16,17,26] Structures **9**, **11**, and **12** in this work are examples thereof. In solution, however, complexes with opposite configuration are sometimes observed (cf. pair **10** and **11**).
2) The methyl ether function of **14** always occupies the position *trans* to a hydride.
3) The imine function binds in a σ fashion *trans* to one of the P atoms. Both steric and electronic effects govern the orientation of DMA-imine on iridium. The orientation is consistent with the relative *trans* influences of the H, N, O and P donors and the requirement that either

the N or the O substituent must fit between two aromatic rings of the phosphorus chelate.

4) It may be assumed that the migratory insertion of the hydride is the enantioselective step. Structures **18** and **20** are at the origin of the observed stereoselectivity of the catalysis (i.e., (*S*)-(*R*)-Xyliphos gives predominantly the (*R*)-amine and vice versa for the actual industrial process). Migratory insertion of the hydrides *cis* to the imine functions in **18** and **20** lead to the postulated Ir^{III} amide intermediates **22** and **23**, respectively, containing a new stereogenic center (Scheme 4). It has been shown that

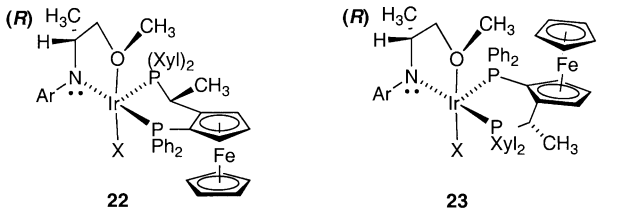

Scheme 4. Proposed intermediates after migratory insertion of the hydrides *cis* to the imine functions in complexes **18** and **20**. X = I, Cl, OAc, HSO_4, H etc. and Ar = 2,6-dimethylaryl or 2-ethyl-6-methylaryl

H_2 readily adds across such Ir^{III}–amide bonds to form a coordinated amine, regenerate an Ir–H function,[27] and thus close the catalytic cycle. Structure **18** (in the real catalytic system, I, Cl, OAc, HSO_4, etc. may actually occupy the position *trans* to the methyl ether function instead of a hydride ligand) should thermodynamically favor migratory insertion to form the new C–H bond due to a synergistic effect caused by the electronic asymmetry of the Xyliphos ligand. In **18** the hydride ligand is more nucleophilic (it is *trans* to the more basic phosphane)[28] and the imine is more electrophilic (it is *trans* to the less basic phosphane) as compared to **19**. Also, the result of the migratory insertion of **18**, the postulated pentacoordinate Ir^{III} amido complex **22**, is expected to be stabilized by the coordination of the highly basic amide function *trans* to the less basic phosphane. On the other hand enantioselectivity could be kinetically controlled, and an analogue of the minor (3%) component **20** may lead to the thermodynamically less stable postulated intermediate **23**. Hydrogenolysis of the iridium–amide bond (in this case *trans* to the more basic phosphane) or amine decoordination would then be the rate-limiting steps. Detailed kinetic studies are necessary at this stage.

Since we were interested in structurally assessing the coordination behavior of the imine **14** by X-ray analysis and since it was not possible to grow X-ray quality single crystals from the mixtures **18**–**21**, we opted for the synthesis of a simple iridium–imine adduct that would display a better crystallinity. The goal was to synthesize an iridium–imine complex with labile spectator ligands that could be easily substituted by diphosphane **4**.[29] When the thermally labile tetraethylene complex **24**[30] was treated with the silver bis-(imine) complex **16** at 195 K, clean metathesis occurred to afford the iridium ethylene DMA imine complex **25** in very good yield [Eq. (4)] along with one equivalent of AgCl and free imine **14**. Complex **16** was obtained as a white powder on a gram scale in excellent yield by treating a solution of $AgBF_4$ in toluene with two equivalents of imine **14**.The ^1H NMR spectrum confirmed the presence of a sole isomer. Broad signals for the ethylene ligands indicated dynamic behavior at room temperature, and the sharp signals for the imine ligand **14** were all shifted to lower fields with respect to those of the free imine. The resonance of the methoxy protons of coordinated **14** was shifted downfield by about 0.5 ppm to $\delta = 3.98$ ppm. The imino methyl protons resonated at $\delta = 1.93$ ppm and the methylene protons at $\delta = 5.49$ ppm, as compared to $\delta = 1.66$ and 4.20 ppm, respectively, in free **14**. The ^1H NMR data thus support a bidentate coordination mode of **14**.[31]

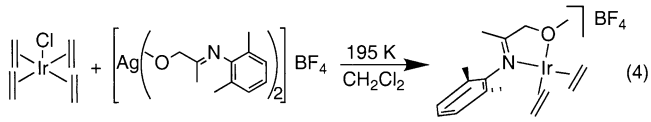

(4)

Crystals of **25** were grown from a CH_2Cl_2/Et_2O mixture and an X-ray diffraction study was performed. The unit cell contains two independent molecules. Figure 7 confirms the κ^2 coordination mode of imine **14**,[32] which has a bite angle of 78°, and a square-planar coordination environment around the iridium center. The iridium atom lies 0.01 Å from the best plane fitted through the N and O atoms of **14** and the midpoints of the ethylene ligands. Similarly, the

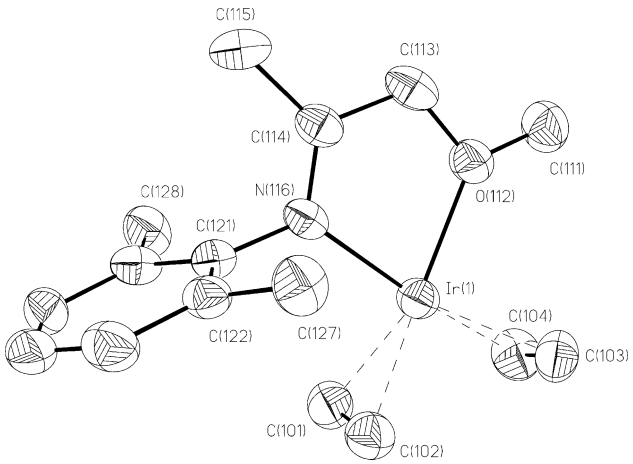

Figure 7. Structure of one of the two independent cations of **25** (ORTEP plot; 30% probability ellipsoids). Selected bond lengths [Å] and angles [°]: Ir(1)–N(116) 2.060(8), Ir(1)–O(112) 2.093(7), Ir(1)–C(102) 2.083(12), Ir(1)–C(101) 2.091(12), Ir(1)–C(103) 2.081(11), Ir(1)–C(104) 2.112(13), N(116)–C(114) 1.288(12), N(116)–C(121) 1.445(12), C(111)–O(112) 1.446(12), C(113)–O(112) 1.406(12), C(114)–C(115) 1.519(13), C(114)–C(113) 1.466(13), C(101)–C(102) 1.399(17), C(103)–C(104) 1.387(15), N(116)-Ir(1)-O(112) 77.7(3), N(116)-Ir(1)-C(102) 97.2(4), O(112)-Ir(1)-C(103) 90.8(4), C(101)-Ir(1)-C(104) 86.7(5).

DMA backbone lies well within the plane defined by Ir, O, and N, with the *ipso*-C(221) atom of the aryl group showing the largest deviation of 0.05 Å. The dihedral angle between the N,O,Ir plane and the plane fitted through the six C atoms of the aryl ring is 87°. The Ir–N bond length (2.06 Å) lies within the expected range, and the Ir–O distance (2.09 Å) is comparable to the length of an Ir–O single bond.[33] Such tight ether coordination was previously observed in a similar Ir^{I} complex.[34] The C–N distance (1.29 Å) does not indicate any appreciable amount of metal–imine π backbonding.[35]

Attempts to isolate adducts of iridium with the hydrogenation product, that is, model amine **17**, under conditions analogous to those that allowed isolation of **18**–**21** failed. Neither (*R*)- nor (*S*)-**17** reacted cleanly with (*S*)-(*R*)-**8** under H_2. This is because imine **14** is a much better ligand for iridium than amine **17**.[36] Note that amine **17** is a close model of MEA-amine (**2**). Complex (*S*)-(*R*)-**13** reacted with amine (*R*)-**17** to form complicated mixtures of hydrides. We showed that chloro-bridged iridium complexes closely related to **13** cleanly react with LiHNPh to afford Ir^{I} amido complexes and Ir^{I} bis-amidate Li salts of the general formulae $[\{(\widehat{PP})Ir(\mu\text{-}HNPh)\}_2]$ and $[(\widehat{PP})Ir(HNPh)_2]Li$, respectively.[37] This prompted us to probe the reactivity of complex **13** with various amounts of the corresponding lithium amide of **17** (obtained by deprotonation of **17** with LiBu) in $[D_8]$THF. Unfortunately, only complicated mixtures of products were obtained. The dinuclear Ir^{III} iodo complex **12** did not react with this lithium amide.

Conclusion

We prepared and characterized a series of complexes that reflect the composition of the "magic catalyst mixture" used in the Syngenta MEA-imine hydrogenation process. Notably, complexes **10** and **11** contain all the ingredients in the coordination sphere of iridium, namely, Xyliphos (**4**), iodide, and a hydride originating from a Brønstedt acid. Not surprisingly, these compounds, along with the unprecedented dinuclear iodo bridged Ir^{III} complex **12**, were the best single-component catalysts for the hydrogenation of imine **1**. The last-named complex is an excellent catalyst precursor even though it does not have an Ir^{III}–H bond. Coordination of imine **14** [a close model for MEA-imine (**1**)] to **8** under 1 bar H_2 pressure was not diastereoselective and led to a mixture of two major (**18**, **19**) and two minor isomers (**20**, **21**). Two of them (**18** and **20**) were in accord with the stereochemical outcome of the catalysis, and migratory insertion leads to the postulated thermodynamic (**22**) or kinetic (**23**) intermediates. Finally, we proved by an X-ray structure analysis of model compound **25** that imine **14** coordinates in an κ^2 fashion to an Ir^{I} center. It was shown that the ether group of the imine binds quite tightly to the iridium center. The coordination behavior of amine **17** on iridium and its exchange kinetics with imine **14** have been the object of investigation in our laboratory and will be reported in due course.[36]

Experimental Section

General aspects: All experiments were performed under purified N_2 in a MBraun glovebox or under purified Ar using standard Schlenk techniques. All glassware and stirbars were oven-dried at 413 K. Pentane and hexane were distilled from Na/K (50% w/w)/tetraglyme/benzophenone, THF and diethyl ether from Na/K, benzene from Na/benzophenone, toluene and heptane from Na, and CH_2Cl_2 from Pb/Na alloy (Aldrich). Acetone (Merck, puriss. p.a.) was dried over activated (553 K, 0.001 mbar, 12 h) 4 Å molecular sieves. C_6D_6 and $[D_8]$THF were dried over Na/K, and CD_2Cl_2 and $CDCl_3$ over Na/Pb alloy. The solvents were freshly distilled before use or kept in dispenser flasks in the glovebox. NMR spectra were recorded on Bruker AC250 and Bruker dpx250 spectrometers (same magnet, ^{1}H: 250.133 MHz, ^{31}P: 101.256 MHz). Chemical shifts are given in ppm relative to internal TMS and to external H_3PO_4 (85%). Coupling constants *J* are reported in hertz. Elemental analyses (EA) were carried out at the Mikroelementaranalytisches Laboratorium at ETH Zurich. All reactions involving silver salts were carried out in the dark. The synthesis of enantiopure (*R*)-**17** will be reported elsewhere.[26] (*R*)-**17** and (*S*)-**17** were also obtained by separation on a preparative-scale chiral Daicel OD-H column.

Bis(3,5-xylyl)phosphane (5): A slightly turbid, yellowish solution of 3,5-dimethylphenyllithium (9.25 g, 82.5 mmol) in Et_2O (150 mL) was added dropwise at 203 K to a colorless solution of $PCl_2(NEt_2)$ (7.18 g, 41.3 mmol) in Et_2O (150 mL). The mixture was allowed to reach room temperature. Then HCl(g) (ca. 160 mmol, liberated by treating 8.5 g of NH_4Cl with H_2SO_4) was slowly bubbled through the vigorously stirred solution. The white precipitate was filtered off and the yellowish solution pumped down. Fresh Et_2O (50 mL) was added, and the resulting solution was added dropwise to a slurry of $LiAlH_4$ (5.56 g, 147 mmol) in Et_2O (150 mL) at 195 K. This mixture was warmed to room temperature over 4 h and stirred overnight. Refluxing for 2 h reflux, filtration, extraction of the gray residue with Et_2O, and subsequent evaporation of the combined Et_2O solutions gave a yellowish oil and a white precipitate. Distillation ($T_{bath} \approx 430$ K; $T_{vap} \approx 398$–405 K; $p \approx 0.04$ mbar) gave 5.89 g (59%) of a yellowish oil. ^{31}P NMR ($CDCl_3$): $\delta = -40.0$ ppm (s).

(*S*)-(*R*)-Xyliphos ((*S*)-1-[(*R*)-2-(diphenylphosphanyl)ferrocenyl]ethyl-bis(3,5-xylyl)phosphane, (*S*)-(*R*)-4): An orange-red solution of (*S*)-*N*,*N*-dimethyl-1-[(*R*)-2-(diphenylphosphany)ferrocenyl]ethylamine (**6**, 8.86 g, 20.1 mmol) in AcOH (160 mL) was degased by two freeze–pump–thaw cycles. Then $PH(3,5\text{-}Xyl)_2$ (**5**, 5.35 g, 22.1 mmol) was added and the mixture was heated to 370 K for 3 h. The volatile substsances were removed in vacuo at 370 K, and EtOH (800 mL) was added to afford a limpid orange solution at reflux temperature. Concentration to 400 mL, filtration, and washing with cold EtOH yielded 9.55 g (69%) of a yellow microcrystalline solid. From the mother liquor another crop of crystals was recovered (0.80 g, 6%). Elemental analysis calcd (%) for $C_{40}H_{40}P_2Fe\cdot C_2H_6O$: C 73.68, H 6.77; found: C 73.54, H 6.80. ^{1}H NMR ($CDCl_3$): $\delta =$ 1.46 (m, 3H), 2.19 (s, 6H), 2.27 (s, 6H), 3.72 (m, 1H), 3.84 (s, 5H), 4.03 (m, 2H), 4.24 (m, 1H), 6.77 (m, 1H), 6.85–7.00 (m, 5H), 7.10–7.20 (m, 5 H), 7.35–7.45 (m, 3H), 7.60–7.70 ppm (m, 2H). The spectrum indicated one equivalent of EtOH of cocrystallization. $^{31}P\{^1H\}$ NMR ($CDCl_3$): $\delta =$ −25.2 (d, $J = 19$ Hz), 6.5 ppm (d, $J = 19$ Hz).

[Ir(Cl)(cod){(*S*)-(*R*)-Xyliphos)}] (7): Warm toluene (50 mL) was added to $[Ir_2(\mu\text{-}Cl)_2(cod)_2]$ (417 mg, 0.621 mmol) and (*S*)-(*R*)-Xyliphos ((*S*)-(*R*)-**4**, 794 mg, 1.244 mmol), and the resulting limpid orange solution was stirred overnight. The volatile substances were evaporated and the remaining orange glassy solid was treated with diethyl ether (20 mL) to give a yellow crystalline solid. The mother liquor was filtered off and the solid dried in vacuo. Yield: 950 mg (78%). Elemental analysis calcd (%) for $C_{48}H_{52}ClFeIrP_2$: C 59.17, H 5.38; found: C 58.95, H 5.57. ^{1}H NMR (C_6D_6): $\delta = 1.70$–1.85 (m, 2H), 1.83 (m, 3H), 2.10–2.30 (m, 2H), 2.12 (m, 6H), 2.19 (m, 6H), 2.35–2.55 (m, 2H), 2.55–2.75 (m, 2H), 3.78 (m, 1H), 3.85–4.10 (m, 4H), 3.96 (s, 5H), 4.42 (m, 2H), 6.45–7.05 (m, 8H), 7.20–7.30 (m, 2H), 7.30–7.40 (m, 2H), 7.82 (br, 2H), 8.86 ppm (m, 2H); ^{31}P NMR (C_6D_6): $\delta = -14.5$ (d, $J = 37$ Hz), 16.4 (d, $J = 37$ Hz). $[\alpha]_D^{20} = 144$ ($c = 0.78$, THF).

[Ir(cod)((*S*)-(*R*)-Xyliphos)]BF_4 (8): An orange solution of $[Ir_2(\mu\text{-}Cl)_2(cod)_2]$ (0.976 g, 1.45 mmol) and (*S*)-(*R*)-Xyliphos ((*S*)-(*R*)-**4**, 1.856 g, 2.91 mmol) in THF (130 mL) was stirred for 0.5 h (slightly turbid). Then

$AgBF_4$ (0.570 g, 2.93 mmol) was added, and the resulting deep red mixture was stirred overnight. The finely divided white precipitate was allowed to settle at 253 K for 2 h. The mother liquor was then decanted off over a Celite filterstick and stripped to a deep red glassy solid. Slurrying and washing with *n*-hexane (25 mL) and drying in vacuo yielded a brick-red powder (2.73 g, 92%). Elemental analysis calcd (%) for $C_{48}H_{52}BF_4FeIrP_2$: C 56.21, H 5.11; found: C 56.12, H 5.20; ^{31}P NMR (C_6D_6): $\delta = 3.2$ (d, $J = 24$ Hz, P1), 37.9 ppm (d, $J = 24$, P2). ^{13}C NMR (CD_2Cl_2): $\delta = 14.52$ (d, $J = 6.0$ Hz, C7), 21.45 (s, C14, C15), 21.70 (s, C22, C23), 28.05 (dd, $J = J = 1.6$, 1.6 Hz, C42), 28.49 (dd, $J = 1.6$, 1.8 Hz, C38), 33.02 (dd, $J = 26.0$, 4.2 Hz, C6), 33.38 (dd, $J = 4.5$, 2.2 Hz, C39), 33.68 (dd, $J = 4.5$, 2.3 Hz, C43), 68.75 (d, $J = 8.0$ Hz, C4), 69.63 (dd, $J = 8.5$, 1.6 Hz), 70.97 (s, C1′–C5′), 73.27 (dd, $J = 54.7$, 5.9 Hz, C1), 74.94 (d, $J = 5.7$ Hz, C5), 84.74 (d, $J = 10.8$ Hz, C36), 85.96 (d, $J = 10.1$ Hz, C40), 89.42 (dd, $J = 18.9$, 4.1 Hz, C2), 91.21 (d, $J = 10.5$ Hz, C37), 92.25 (d, $J = 11.1$ Hz, C41), 127.15 (dd, $J = 44.7$ Hz, 0.9, C_{ipso}), 127.37 (d, $J = 50.8$ Hz, C_{ipso}), 128.89 (d, $J = 10.0$, C32 Hz, C34), 129.01 (dd, $J = 55.6$, 1.1 Hz, C_{ipso})), 129.48 (d, $J = 5.6$ Hz, C17, C21), 129.56 (d, $J = 8.5$ Hz, C25, C29), 131.44 (d, $J = 2.4$ Hz, C33), 132.85 (d, $J = 2.5$ Hz, C27), 133.01 (d, $J = 9.2$ Hz, C31, C35), 133.38 (d, $J = 2.5$ Hz, C19), 134.29 (d, $J = 11.3$ Hz, C9, C13), 134.37 (d, $J = 2.6$ Hz, C11), 135.10 (d, $J = 56.5$ Hz, C_{ipso}), 136.83 (d, $J = 13.5$ Hz, C24), 138.77 (d, $J = 11.1$ Hz, C10, C11), 139.45 ppm (d, $J = 9.9$ Hz, C18, C20); ^{1}H NMR (CD_2Cl_2): $\delta = 1.50$ (dd, 3 H7), 1.56 (m, H42), 1.61 (m, H38), 1.66 (m, H42), 1.88 (m, H38), 2.06 (m, H43), 2.30 (s, 3 H14, 3 H15), 2.32 (m, H43), 2.34 (m, 2 H39), 2.40 (s, 3 H22, 3 H23), 3.28 (m, H41), 3.60 (dq, H6), 3.65 (m, H37), 3.73 (s, H1′–H5′), 4.03 (m, H3), 4.15 (dt, H4), 4.19 (m, H36), 4.20 (m, H40), 4.33 (td, H5), 7.04 (md, H17, H21), 7.19 (m, H19), 7.20 (m, H11), 7.34 (md, H9, H13), 7.37 (m, H31, H35), 7.51 (m, H33), 7.52 (m, H32, H34), 7.77 (m, H27), 7.81 (m, H26, H28), 8.35 ppm (m, H25, H29). Single crystals suitable for X-ray diffraction analysis were grown from a saturated, filtered solution of the complex in THF.

[Ir(I)(cod)((*S*)-(*R*)-Xyliphos)] (9): Acetone (150 mL) was added to $[Ir_2(\mu\text{-}Cl)_2(cod)_2]$ (0.959 g, 1.428 mmol), (*S*)-(*R*)-Xyliphos ((*S*)-(*R*)-**4**, 1.823 g, 2.855 mmol), and KI (0.498 g, 3.002 mmol). Stirring for 3 h afforded a yellow slurry, which was pumped down. Toluene (150 mL) was added and the mixture was filtered over Celite. The volatile substances were removed in vacuo leaving an orange glassy solid. Washing with hexane and drying in vacuo yielded a yellow powder (2.81 g, 92%). Elemental analysis calcd (%) for $C_{48}H_{52}P_2FeIIr$: C 54.09, H 4.92; found: C 54.34, H 5.08; ^{31}P NMR (C_6D_6): $\delta = -24.0$ (d, $J = 41$ Hz, P1), 7.5 ppm (d, $J = 41$ Hz, P2); ^{13}C NMR (C_6D_6): $\delta = 17.09$ (d, $J = 7.4$ Hz, C7), 21.40 (s, Me_{Xyl}), 21.42 (s, Me_{Xyl}), 32.59 (d, $J = 3.7$ Hz, C39, C43), 32.77 (d, $J = 3.5$ Hz, C38, C42), 35.30 (d, $J = 28.1$ Hz, C6), 67.20 (dd, $J = 10.8$, 1.6 Hz, C37, C41), 68.33 (d, $J = 4.9$ Hz, C4), 69.05 (dd, $J = 8.1$, 2.6 Hz, C3), 70.13 (d, $J = 12.5$ Hz, C36, C40), 71.46 (s, C1′–C5′), 73.61 (dd, $J = 47.4$, 7.9 Hz, C1), 74.21 (d, $J = 1.4$ Hz, C5), 94.48 (dd, $J = 18.9$, 5.8 Hz, C2), 126.51 (d, $J = 8.7$ Hz, C32, C34), 127.44 (s, C33), 127.48 (d, $J = 8.3$ Hz, C26, C28), 130.37 (d, $J = 2.3$ Hz, C27), 131.55 (br, C9, C13), 131.93 (d, $J = 2.4$ Hz, C19), 131.96 (d, $J = 2.3$ Hz, C11), 132.49 (dd, $J = 40.5$, 3.9 Hz, C_{ipso}), 133.51 (d, $J = 8.0$ Hz, C31, C35), 134.60 (dd, $J = 44.1$, 2.2 Hz, C_{ipso}), 135.20 (br, C17, C21), 136.35 (d, $J = 10.3$ Hz, C25, C29), 137.09 (br, C10, C12), 137.51 (d, $J = 10.0$ Hz, C18, C20), 140.65 (d, $J = 51.2$ Hz, C_{ipso}), one C_{ipso} masked by C_6D_6, 127.16 ppm (dd, $J = 44.6$, 1.6 Hz) in $CDCl_3$). ^{1}H NMR (C_6D_6): $\delta = 1.79$ (dd, 3 H7), 1.96 (m, H38, H42), 2.01 (s, 3 H22, 3 H23), 2.03 (m, H39, H43), 2.14 (br, 3 H14, 3 H15), 2.53 (m, H39, H43), 2.65 (m, H38, H42), 3.67 (m, H36, H40), 3.80 (m, H5), 3.84 (m, H4), 4.06 (s, H1′-H5′), 4.26 (m, H37, H41), 4.35 (m, H3), 6.65 (m, H31, H35), 6.68 (qd, H6), 6.74 (m, H11), 6.78 (m, H32, H34), 6.83 (m, H19), 6.97 (m, H33), 7.15 (m, H27), 7.27 (m, H26, H28), 7.50 (md, H17, H21), 8.75 ppm (m, H25, H29), H9 and H13 too broad to be observed (7.2 in $CDCl_3$ with $\Delta_{1/2} = 150$ Hz). Single crystals suitable for X-ray diffraction analysis were obtained as follows: 150 mg of the complex was dissolved in THF (7 mL), Et_2O was added to just induce precipitation, and subsequent warming redissolved the precipitate. The resulting limpid solution was allowed to slowly cool to room temperature.

[Ir(H)(I)(cod)((*S*)-(*R*)-Xyliphos)]BF_4·CH_2Cl_2 (10): A solution of HBF_4 in Et_2O (54 wt%, $d = 1.19$, 26 μL, ca. 0.19 mmol) was slowly added to a red solution of [Ir(I)(cod)((*S*)-(*R*)-Xyliphos)] (**9**, 203 mg, 0.191 mmol) in CH_2Cl_2 (10 mL) at 195 K. The solution turned yellow and was allowed to slowly reach room temperature. The resulting orange solution was stripped to a red oily solid, which was redissolved in fresh CH_2Cl_2 (1 mL). Dropwise addition of Et_2O (4 mL) caused the precipitation of a brick-red solid. The mother liquor was syphoned off, and the solid washed with Et_2O (4 mL) and dried in vacuo to give a pink powder (98 mg, 41%). Elemental analysis calcd (%) for $C_{48}H_{53}BF_4FeIIrP_2$·CH_2Cl_2: C 47.52, H 4.48,I 10.25; found: C 47.91 , H 4.42, I 10.34; IR: $\tilde{\nu}$(IrH) = 2259 cm^{-1} (CsI). ^{31}P NMR (CD_2Cl_2): δ −12.4 (d, $J = 18$ Hz), 23.5 ppm (d, $J = 18$ Hz); ^{13}C NMR (CD_2Cl_2): $\delta = 13.80$ (d, $J = 5.6$ Hz, C7), 21.73 (s, C14, C15), 21.78 (s, C22, C23), 31.69 (dd, $J = 3.8$, 0.9 Hz, *), 31.75 (dd, $J = 4.3$, 2.2 Hz, *), 32.08 (dd, $J = 3.4$, 1.0 Hz, *), 32.21 (4.1, 2.5 Hz, *), 37.64 (dd, $J = 26.3$, 4.1 Hz, C6), 69.48 (d, $J = 9.4$ Hz, C4), 71.49 (s, C1′-C5′), 71.50 (dd, $J = 9.0$, 1.0 Hz, C3), 75.95 (d, $J = 6.3$ Hz, C5), 89.16 (dd, $J = 7.6$, 0.9 Hz, C37), 90.83 (dd, $J = 8.1$, 1.4 Hz, C42), 95.81 (d, $J = 15.3$ Hz, C38), 98.95 (d, $J = 15.3$ Hz, C41), 125.83 (d, $J = 51.2$ Hz, C_{ipso}), 126.52 (dd, $J = 59.4$, 1.0 Hz, C_{ipso}), 127.22 (d, $J = 53.3$ Hz, C_{ipso}), 128.41 (d, $J = 10.9$ Hz, C26, C28), 129.45 (d, $J = 10.7$ Hz, C32, C34), 131.20 (d, $J = 60.7$ Hz, C_{ipso}), 131.70 (d, $J = 9.4$ Hz, C9, C13), 132.04 (d, $J = 6.3$ Hz, C17, C21), 132.72 (d, $J = 2.8$ Hz, C27), 133.28 (d, $J = 2.6$ Hz, C33), 133.77 (d, $J = 2.9$ Hz, C19), 134.46 (d, $J = 2.6$ Hz, C11), 134.7 (br, C25, C29), 135.2 (br, C31, C35), 137.48 (d, $J = 10.9$ Hz, C10, C12 or C18, C20), 139.56 ppm (d, $J = 10.9$ Hz, C18, C20 or C10, C12); * = C39, C40, C43, C44, not specifically assigned. ^{1}H NMR (CD_2Cl_2): $\delta = -12.58$ (dd, $J = 10.7$, 10.7 Hz, IrH), 1.52 (dd, 3 H6), 2.29 (s, 3 H18, 3 H20), 2.32 (m, H39), 2.41 (s, 3 H10, 3 H12), 2.43 (m, H40), 2.44 (m, H43), 2.52 (m, H44), 2.53 (m, H43), 2.67 (qd, H6), 2.73 (2 m, H39, H40), 2.81 (m, H44), 3.94 (m, H38), 3.99 (s, H1′-H5′), 4.15 (m, H41), 4.71 (2 m, H4, H5), 4.76 (m, H37), 4.83 (m, H42), 4.91 (m, H3), 6.90 (md, H17, H21), 7.10 (m, H19), 7.26 (m, H11), 7.44 (m, H26, H28), 7.53 (m, H27), 7.56 (md, H9, H13), 7.79 (m, H33), 7.84 (m, H32, H34), 7.85 (vbr, H25, H29), 8.75 ppm (m, H31, H35).

[Ir(I)(H)(cod)((*S*)-(*R*)-Xyliphos)]BF_4·0.5CH_2Cl_2 (11): A solution of HBF_4 in Et_2O (54 wt%, $d = 1.19$, 260 μL, 1.90 mmol) was slowly added to a deep red solution of [Ir(I)(cod)((*S*)-(*R*)-Xyliphos)] (**9**, 1.015 g, 0.952 mmol) in CH_2Cl_2 (40 mL), and the mixture stirred for 60 h. Concentration (4 mL), addition of Et_2O (16 mL), and stirring overnight caused the formation of a yellow microcrystalline precipitate. After standing at 253 K for 4 h, the deep red mother liquor was decanted off, and the solid washed with Et_2O (30 mL) and dried in vacuo to yield an orange powder (660 mg, 58%). From the mother liquor another crop of crystals was recovered (68 mg, 6%). Elemental analysis calcd (%) for $C_{48}H_{53}BF_4FeIIrP_2$·0.5CH_2Cl_2: C 48.70, H 4.55, I 10.61; found: C 48.76, H 4.67, I 10.87; IR: $\tilde{\nu}$(IrH) = 2256 cm^{-1} (CsI); ^{31}P{H} NMR (CD_2Cl_2): $\delta = -31.9$ (d, $J = 23$ Hz), −1.5 (d, $J = 23$); ^{13}C NMR (CD_2Cl_2): $\delta = 16.02$ (br, C7), 21.56, 21.58, 21.61 (3 s, 4 Me_{Xyl}), 30.33 (m, C44), 30.49 (m, C40), 32.40 (d, $J = 2.8$ Hz, C43), 33.78 (m, C39), 34.37 (d, $J = 33.3$ Hz, C6), 69.55 (dd, $J = 64.2$, 6.1 Hz, C1), 70.34 (br, C4), 71.20 (br, C3), 72.44 (br, C1′–C5′), 74.54 (br, C5), 91.38 (br, C42), 94.13 (d, $J = 7.7$ Hz, C37), 97.75 (d, $J = 13.5$ Hz, C38), 99.36 (d, $J = 11.8$ Hz, C41), 124.80 (d, $J = 55.9$ Hz, C_{ipso}), 126.43 (d, $J = 49.0$ Hz, C_{ipso}), 128.22 (d, $J = 10.1$ Hz, C26, C28), 128.24 (d, $J = 56.9$ Hz, C_{ipso}), 128.87 (d, $J = 10.7$ Hz, C32,C34), 130.38 (dd, $J = 5$ Hz, 6, C9), 130.66 (s, C27), 130.87 (d, $J = 9.9$ Hz, C13), 131.20 (d, $J = 9.1$ Hz, C25, C29), 132.18 (m, C17, C21), 132.81 (d, $J = 2.2$ Hz, C33), 134.31 (m, C11), 134.43 (m, C19), 134.90 (d, $J = 9.5$ Hz, C31, C35), 139.04 (d, $J = 10.3$ Hz, C10 or C12), 139.11 (d, $J = 65.2$ Hz, C_{ipso}), 139.14 (d, $J = 11.7$ Hz, C12 or C10), 139.72 ppm (d, $J = 10.9$ Hz, C32, C34); ^{1}H NMR (CD_2Cl_2): $\delta = -13.84$ (dd, $J = 15.8$, 9.2 Hz, IrH), 1.61 (dd, 3 H7), 2.10 (s, 3 H14), 2.19 (s, 3 H22, 3 H23), 2.39 (3 m, H40, 2 H44), 2.46 (s, 3 H15), 2.47 (m, H43), 2.62 (m, H43), 2.98 (m, H39), 3.02 (m, H40), 3.42 (m, H39), 3.86 (m, H5), 4.12 (H1′–H5′), 4.26 (m, H41), 4.43 (m, H4), 4.55 (m, H42), 4.92 (m, H3), 5.13 (m, H37), 5.51 (m, H38), 6.10 (md, H9), 6.46 (m, H25, H29), 6.48 (qd, H6), 7.03 (m, H26, H28), 7.04 (md, H17, H21), 7.10 (m, H11), 7.11 (m, H19), 7.29 (m, H27), 7.57 (m, H32, H34), 7.62 (m, H33), 8.34 (md, H13), 8.35 ppm (m, H31, H35). Single crystals suitable for X-ray diffraction analysis were grown from a filtered solution of 82 mg complex in CH_2Cl_2 (0.3 mL) and THF (0.6 mL).

[Ir_2I_2(μ-I)$_3$((*S*)-(*R*)-Xyliphos)$_2$]I (12): A solution of I_2 (72.23 mg, 0.2845 mmol) in toluene (20 mL) was added dropwise to a stirred solution of [Ir(I)(cod)((*S*)-(*R*)-Xyliphos)] (**9**, 303.3 mg, 0.2845 mmol) in toluene (30 mL) at 203 K. The resulting dark red solution was allowed to slowly reach room temperature. Then it was heated at 323 K for 0.5 h. The solution turned red-brown and a small amount of an oily precipitate formed. After evaporation of the volatile substances the residue was washed and slurried with hexane (2 × 60 mL). Drying in vacuo afforded a

brown powder (276 mg, 80%). Elemental analysis calcd (%) for $C_{80}H_{80}Fe_2I_6Ir_2P_4$: C 39.66, H 3.33, I 31.43; found: C 39.52, H 3.07, I 31.37; ^{1}H NMR (CD_2Cl_2): $\delta = 1.15$ (m, 6H), 1.81 (s, br, 12H), 2.05 (s, br, 6H), 2.12 (s, br, 6H), 3.76 (s, 10H), 4.47 (m, 2H), 4.55 (m, 2H), 4.86 (s, 2H), 5.19 (m, 2H), 6.35 (m, 4H), 6.69 (m, 4H), 6.87 (s, 2H), 7.01 (s, 2H), 7.16 (m, 2H), 7.20–7.70 (m, br, 12H), 8.40 (m, 2H), 8.61 ppm (m, 4H); ^{31}P{H} NMR (CD_2Cl_2/C_6D_6): $\delta = -22.0$ (d, $J = 11$ Hz), 2.0 ppm (d, $J = 11$ Hz). Crystals suitable for X-ray crystallographic analysis were grown from CH_2Cl_2/Et_2O.

***cis*- and *trans*-[Ir$_2$(μ-Cl)$_2$((*S*)-(*R*)-Xyliphos)$_2$] (13)**: A red solution of (*S*)-(*R*)-Xyliphos ((*S*)-(*R*)-**4**, 2.001 g, 3.133 mmol) in benzene (40 mL) was added dropwise over 20 min to a stirred bright orange slurry of [Ir_2Cl_2(coe)$_4$] (1.416 g, 1.566 mmol) in benzene (40 mL) to afford a limpid deep red solution. After stirring for 15 min the solvent was removed in vacuo leaving an orange solid. Washing with pentane and drying in vacuo afforded a yellow powder (2.40 g, 88%). Elemental analysis calcd (%) for $C_{80}H_{80}Cl_2Fe_2Ir_2P_4$): C 55.46, H 4.65; found: C 55.18, H 4.80; ^{31}P{^{1}H} NMR (C_6D_6), AA′XX′ spin system, two isomers: $\delta = -4.22$ ($^2J_{PP'} + {}^4J_{PP'} = 38.3$ Hz, isomer A), −1.01 ($^2J_{PP'} + {}^4J_{PP'} = 30.6$ Hz, isomer B), 22.70 ($^2J_{PP'} + {}^4J_{PP'} = 38.2$ Hz, isomer A), 26.73 ppm ($^2J_{PP'} + {}^4J_{PP'} = 30.6$ Hz, isomer B); ^{1}H NMR (C_6D_6): $\delta = 1.05$ −1.20 (m, 6H, isomer A), 1.25–1.35 (m, 6H, isomer B), 2.12 (s, 12H, isomer B), 2.17 (s, 12H, isomer B), 2.22 (s, 12H, isomer A), 2.38 (s, 12H, isomer A), 3.57 (s, 10H, isomer B), 3.68 (s, 10H, isomer A), 3.75–4.20 (m, 8H, isomers A and B), 6.75 −8.55 ppm (m, 32 H, isomers A and B).

Typical hydrogenation protocol: MEA-imine (20.5 mL, 0.1 mol) was transferred under argon to a magnetically stirred 50 mL steel autoclave containing (*R*)-(*S*)-**12** (2.4 mg, 0.001 mmol). The autoclave was purged five times with 5 bar H_2 (99.5%) and finally pressurized to 100 bar (this pressure was maintained throughout the experiment). Stirring at 1500 rpm and warming to 303 K initiated the hydrogenation reaction, which was left for 18 h. The reaction solution was diluted in CH_2Cl_2 (1% v/v) and analyzed by GC (Varian 3700, OV-101 column, temperature program: $T_{init} = 373$ K, 10 K min^{-1} up to 593 K; retention times: MEA-amine 8.05 min, MEA-imine 7.65 min); 75.0% yield of MEA-amine **2**. The *ee* was determined by HPLC on a Daicel Chiracel OD-H column with hexane/*i*PrOH (99.65/0.35) as eluent (1.0 mL min^{-1}; 298 K; retention times: (*R*)-**2** 6.9 min, (*S*)-**2** 8.0 min; 79% *ee* (*S*)).

DMA-imine (2,6-dimethylphenyl-1′-methyl-2′-methoxyethyl-imine, 14): A mixture of methoxyacetone (41.2 g, 467 mmol) and 2,6-dimethylaniline (57.9 g, 478 mmol) in toluene (100 mL) was heated to reflux on a water separator for 24 h. About 8.5 mL of H_2O was collected. The volatile substances were evaporated. Acetic anhydride (3.6 mL, 38 mmol) was added to the yellowish residue to scavenge excess 2,6-dimethylaniline, and the mixture was stirred at room temperature overnight. Fractionation (70–74 °C, 0.007 mbar) yielded a yellowish oil (71 g, 79%). Elemental analysis calcd (%) for $C_{12}H_{17}NO$: C 75.35, H 8.96, N 7.32; found: C 75.00, H 9.10, N 7.25; ^{1}H NMR (250.13 MHz, $CDCl_3$): $\delta = 1.66$ (s, 3H, *E* isomer); 2.00 (br s, 6H, both isomers); 2.29 (s, 3H, *Z* isomer); 3.25 (s, 3H, *Z* isomer); 3.48 (s, 3H, *E* isomer); 3.62 (s, 2H, *Z* isomer); 4.20 (s, 2H, *E* isomer); 6.85–6.90 (m, 1H, both isomers); 6.95–7.00 ppm (m, 2H, both isomers). $Z:E \approx 0.16$.

2,6-Dimethylphenyl-1′-methyl-2′-methoxyethyliminium tetrafluoroborate (15). A solution of HBF_4 (54 wt% in Et_2O, 3.50 mL, 25.7 mmol) was added dropwise to a solution of DMA-imine (**14**, 4.92 g, 25.7 mmol) in Et_2O (125 mL) at −40 °C. A white flocculating solid formed, and the mixture was left stirring overnight to slowly reach room temperature. The supernatant was filtered off, and the residue washed with Et_2O (2 × 50 mL) and dried in vacuo affording a white powder (6.74 g, 94%). ^{1}H NMR (250.13 MHz, CD_2Cl_2): $\delta = 2.22$ (s, 6H), 2.39 (s, 3H), 3.67 (s, 3H), 4.85 (s, 2H), 7.20–7.30 (m, 2H), 7.35–7.45 (m, 1H), 11.90 ppm (br, 1H).

[Ag(DMA-Imine)$_2$]BF$_4$ (16): DMA-imine (**14**, 5.5 mL, 28.2 mmol) was added by syringe to a solution of $AgBF_4$ (1.11 g, 5.70 mmol) in toluene (120 mL). After stirring at room temperaure for 3 h a white precipitate formed. The mother liquor was filtered off and the solid dried in vacuo overnight. Washing the solid with pentane (2 × 60 mL) and drying in vacuo afforded an off-white solid (2.96 g, 90%). Elemental analysis calcd (%) for $C_{24}H_{34}N_2BO_2F_4Ag$: C 49.94, H 5.94, N 4.85; found: C 50.19, H 6.04, N 4.81; ^{1}H NMR (250.13 MHz, CD_2Cl_2): $\delta = 1.69$ (s, 3H); 1.99 (s, 6 H); 3.23 (s, 3H); 4.22 (s, 2H); 7.08–7.10 ppm (m, 3H).

[Ir(H)$_2$((*S*)-(*R*)-Xyliphos)(DMA-imine)]BF$_4$ (18, 19, 20, 21): A stream of H_2 ($p \approx 2$ bar) was slowly bubbled for 0.2 h through a deep red solution of [Ir(cod)((*S*)-(*R*)-Xyliphos)]BF_4 (**8**, 76.9 mg, 0.0750 mmol) and DMA-imine **14** (143 mg, 0.75 mmol) in CH_2Cl_2 (7.5 mL). The solution turned orange within seconds. Then the solution was pumped down to an orange oil. Treatment of the oil with pentane (10 mL) afforded a pale yellow powder, which was washed with another portion of pentane and dried in vacuo (65 mg, 75%). Elemental analysis calcd (%) for $C_{52}H_{59}BF_4FeIrNOP_2 \cdot 0.5CH_2Cl_2$: C 54.67, H 5.24, N 1.21; found: C 54.94, H 5.35, N 1.21; **18**: ^{31}P NMR (CD_2Cl_2): $\delta = -4.4$ (d, $J = 8.5$ Hz, P1), 23.2 ppm (d, $J = 8.5$ Hz, P2); ^{13}C NMR (CD_2Cl_2): $\delta = 15.33$ (d, $J = 5.7$ Hz, C7), 17.17 (s, C47), 17.96 (d, $J = 2.4$, C38), 20.71 (d, $J = 2.2$, C46), 21.39 (s, C22, C23), 21.75 (s, C14, C15), 38.16 (dd, $J = 27.3$, 2.1, C6), 61.26 (s, C39), 69.65 (d, $J = 6.8$, C4), 71.18 (s, C1′–C5′), 71.4 (C3), 74.61 (d, $J = 3.5$, C5), 83.17 (dd, $J = 1.2$, 1.2, C37), 95.24 (dd, $J = 17.8$, 3.7), aromatic C atoms not assigned, 180.64 (dd, $J = 2.4$, 1.0, C37). ^{1}H NMR (CD_2Cl_2): $\delta = -29.86$ (ddd, $J = 24.7$, 13.5, 4.8, IrH), −6.95 (ddd, $J = 147.2$, 21.8, 4.8, IrH), 0.99 (dd, $J =$ H7), 1.25 (s, 3 H47), 1.37 (s, 3 H39), 1.60 (s, 3 H38), 2.09 (s, 3 H14, 3 H15), 2.23 (s, 3 H22, 3 H23), 2.67 (s, 3 H46), 3.38 (qd, H6), 3.50 (s, H1′–H5′), 4.02 (d, $J = 36$ Hz), 4.45 (2 m, H4, H5), 4.48 (d, $J = 36$ Hz), 4.79 (m, H3), *ortho*-protons: 6.81 (md, H31, H35), 7.00 (md, H17, H21), 7.23 (m, H25, H29), 8.06 ppm (md, H9, H13); **19**: ^{31}P NMR (CD_2Cl_2): $\delta = 2.6$ (d, $J = 8.5$ Hz, P1), 11.9 ppm (d, $J = 8.5$ Hz, P2); ^{13}C NMR (CD_2Cl_2): $\delta = 16.87$ (d, $J = 5.7$ Hz, C7), 17.67 (d, $J = 2.8$ Hz, C38), 18.01 (s, C47), 20.79 (d, $J = 2.6$ Hz, C46), 21.53 (s, C14, C15, C22, C23), 36.04 (dd, $J = 33.9$, 1.9 Hz, C6), 62.75 (s, C39), 69.47 (d, $J = 5.6$ Hz, C4), 71.0 (C3), 71.03 (s, C1′–C5′), 75.02 (d, $J = 1.3$ Hz, C5), 82.72 (d, $J = 1.9$ Hz, C37), 93.59 (dd, $J = 19.4$, 2.5 Hz, C2), aromatic C atoms not assigned, 180.00 ppm (dd, $J = 2.5$, 1.2 Hz, C37); ^{1}H NMR (CD_2Cl_2): $\delta = -30.19$ (ddd, $J = 25.6$, 12.6, 4.8 Hz, Ir–H), −6.14 (ddd, $J = 150.1$, 19.3, 4.8 Hz, IrH), 1.14 (dd, $J = 7$ Hz), 1.30 (s, 3 H47), 1.67 (s, 3 H38), 1.71 (s, 3 H39), 2.24 (s, 3 H22, 3 H23), 2.39 (s, 3 H14, 3 H15), 2.71 (s, 3 H46), 3.45 (s, H1′-H5′), 3.52 (qd, H6), 4.16 (m, H5), 4.20 (d, $J =$ H36), 4.41 (m, H4), 4.48 (d, $J =$ H36), 4.73 (m, H3), *ortho*-protons: 7.14 (m, H25, H29), 7.17 (md, H17, H21), 7.43 (m, H31, H35), 7.55 ppm (md, H9, H13); **20**: ^{31}P NMR (CD_2Cl_2): $\delta = 5.4$ (P1), 30.8 (P2); ^{1}H NMR (CD_2Cl_2): $\delta = -30.63$ (ddd, $J = 22.0$, 13.9, 4.5, Ir-H), −7.35 (ddd, $J = 145.2$, 22.0, 4.5 Hz, IrH), 1.19 (dd, 3 H7), *ortho*-protons: 6.59 (H17, H21), 6.98 (H25, H29), 7.30 (H9, H13), 8.16 ppm (H31, H35); **21**: ^{31}P NMR (CD_2Cl_2): $\delta = -1.0$ (P1), 42.1 ppm (P2); ^{1}H NMR (CD_2Cl_2): $\delta = -31.69$ (ddd, $J = 28.7$, 8.5, 5.9 Hz, IrH), −8.06 (ddd, $J = 153.3$, 20.0, 5.9 Hz, IrH), 1.36 (dd, 3 H7), *ortho*-protons: 6.66 (H17, H21), 7.06 (H9, H13), 7.85 (H25, H29), 8.06 ppm (H31, H35).

[Ir(DMA-imine)(C$_2$H$_4$)$_2$]BF$_4$ (25): Ethylene (1 bar) was bubbled through a slurry of [Ir_2(μ-Cl)$_2$(coe)$_4$] (1.044 g, 1.165 mmol) in heptane (5 mL) for 0.2 h at 273 K. The resulting off-white slurry was cooled to 195 K, and pentane (20 mL) was added at this temperature. The supernatant solution was decanted off, and CH_2Cl_2 (10 mL) was added to give a turbid greenish solution. A solution of [Ag(DMA-imine)$_2$]BF_4 (**16**, 1.344 g, 2.328 mmol) in CH_2Cl_2 (10 mL) was then added over 0.2 h at 195 K. The resulting greenish limpid solution was allowed to reach room temperature overnight, and a white finely divided precipitate and an orange supernatant solution formed. This mixture was evaporated to dryness, washed with Et_2O (2 × 30 mL), and extracted with CH_2Cl_2 (3 × 10 mL) over a Celite filterstick. Concentration of the mother liquor to 15 mL and addition of Et_2O precipitated an orange microcrystalline solid, which was filtered off and dried in vacuo (1.08 g, 87%). Elemental analysis calcd (%) for $C_{16}H_{25}BF_4IrNO \cdot 0.5\,CH_2Cl_2$: C 34.84, H 4.61, N 2.46; found: C 35.19, H 4.64, N 2.47; ^{1}H NMR (CD_2Cl_2): $\delta = 1.2$–3.9 (br, 8H), 1.93 (s, 3H), 2.22 (s, 6H), 3.98 (s, 3H), 5.49 (s, 2H), 7.16 ppm (s, 3H). The spectrum indicated the presence of 0.5 equiv of CH_2Cl_2. Crystals suitable for X-ray analysis were grown by vapor diffusion of Et_2O into a CH_2Cl_2 solution that was prepared by first washing 185 mg of the complex in THF (3 mL), drying in vacuo, and then dissolving it in CH_2Cl_2 (2 mL).

CCDC-189331, CCDC-189332, CCDC-189329, CCDC-189330, and CCDC-134961 contain the supplementary crystallographic data for compounds **8**, **9**, **11**, **12**, and **25**, respectively. These data can be obtained free of charge via www.ccdc.cam.ac.uk/conts/retrieving.html (or from the Cambridge Crystallographic Data Centre, 12 Union Road, Cambridge CB2 1EZ, UK; fax: (+44) 1223-336-033; or deposit@ccdc.cam.uk).

Acknowledgement

Drs. Volker Gramlich and Fabio Zürcher are acknowledged for solving the X-ray structures of compounds **8**, **9**, **11**, **12**, and **25**. R.D. thanks Novartis AG (Switzerland) and Fonacit (Venezuela) for financial support.

[1] E. N. Jacobsen, A. Pfaltz, H. Yamamoto, *Comprehensive Asymmetric Catalysis*, Springer, Berlin **1999**.
[2] R. Crabtree, H. Felkin, T. Fellebeen-Kahn, G. Morris, *J. Organomet. Chem.* **1979**, *168*, 183.
[3] Y. Ng Cheong Chan, J. A. Osborn, *J. Am. Chem. Soc.* **1990**, *112*, 9400.
[4] F. Spindler, B. Pugin, H.-U. Blaser, *Angew. Chem.* **1990**, *102*, 561; *Angew. Chem. Int. Ed. Engl.* **1990**, *29*, 558.
[5] D. Xiao, X. Zhang, *Angew. Chem.* **2001**, *113*, 3533–3536; *Angew. Chem. Int. Ed.* **2001**, *40*, 3425–3428.
[6] R. Imwinkelried, *Chimia* **1997**, *51*, 300.
[7] F. Spindler, H.-U. Blaser, *Enantiomer* **1999**, *4*, 557.
[8] C. Vogel, R. Aebi (Ciba-Geigy AG), DP 2328340, **1972**.
[9] H. Moser, G. Rhys, *Z. Naturforsch. Teil B* **1982**, *37*, 451.
[10] H.-U. Blaser, W. Brieden, B. Pugin, F. Spindler, M. Studer, A. Togni, *Top. Catal.* **2002**, *19*, 3.
[11] G. Fink, R. Mühlhaupt, H. H. Brintzinger, *Ziegler Catalysts*, Springer, Berlin Heidelberg **1995**.
[12] R. Noyori, T. Ohkuma, *Angew. Chem.* **2001**, *113*, 40–75; *Angew. Chem. Int. Ed.* **2001**, *40*, 40–73.
[13] T. Hayashi, T. Mise, M. Fukushima, M. Kagotani, N. Nagashima, Y. Hamada, A. Matsumoto, S. Kawakami, M. Konishi, K. Yamamoto, M. Kumada, *Bull. Chem. Soc. Jpn.* **1980**, *53*, 1138.
[14] A. Togni, C. Breutel, A. Schnyder, F. Spindler, H. Landert, A. Tijani, *J. Am. Chem. Soc.* **1994**, *116*, 4062.
[15] W. J. Hälg, L. R. Örström, H. Rüegger, L. M. Venanzi, T. Gerfin, V. Gramlich, *Helv. Chim. Acta* **1993**, *76*, 788.
[16] R. Dorta, A. Togni, *Organometallics* **1998**, *17*, 3423.
[17] R. Dorta, A. Togni, *Organometallics* **1998**, *17*, 5441.
[18] In fact, one would expect **11** to be the product of simple protonation of **9**. Moreover, it is still uncertain whether the isomerization of **10** to **11** is catalytic in HBF_4.
[19] J. Eckert, C. M. Jensen, T. F. Koetzle, T. Le Husebo, J. Nicol, P. Wu, *J. Am. Chem. Soc.* **1995**, *117*, 7271.
[20] H.-J. Steinebach, W. Preetz, *Z. Anorg. Allg. Chem.* **1985**, *530*, 155.
[21] M. J. Burk, B. Segmuller, R. H. Crabtree, *Organometallics* **1987**, *6*, 2241.
[22] P. R. Ellis, J. M. Pearson, A. Haynes, A. Adams, N. A. Bailey, P. M. Maitlis, *Organometallics* **1994**, *13*, 3215.
[23] R. Dorta, P. Egli, F. Zürcher, A. Togni, *J. Am. Chem. Soc.* **1997**, *119*, 10857.
[24] R. Dorta, A. Togni, *Chem. Commun.* **2003**, 760.
[25] Note that the indicated TOFs are average values over 18 h and that, depending on the purity of the MEA-imine, reaction times of less than 2 h for total conversion have been observed.
[26] R. Dorta, Ph.D. thesis Nr. 12739, ETH Zürich, **1998**.
[27] M. D. Fryzuk, P. A. MacNeil, S. J. Rettig, *J. Am. Chem. Soc.* **1987**, *109*, 2803.
[28] D. M. Fryzuk, W. E. Piers, *Organometallics* **1990**, *9*, 986.
[29] This is the reverse of our initial and unsuccessful strategy of treating the imine with preformed iridium Xyliphos complexes **7**–**13**.
[30] A. L. Onderlinden, A. van der Ent, *Inorg. Chim. Acta* **1972**, *6*, 420.
[31] Attempts to produce the homoleptic bis-imine iridium complex by displacing the ethylene ligands with a large excess of imine **14** failed. When **25** was treated with diphosphane **4** in CH_2Cl_2 at 195 K a hydrido species formed, and no free imine **14** was detected in the mother liquor. To date, we have been unable to isolate this compound in pure form.
[32] A. G. Becalski, W. R. Cullen, M. D. Fryzuk, B. R. James, G.-J. Kang, S. J. Rettig, *Inorg. Chem.* **1991**, *30*, 5002.
[33] C. A. Miller, T. S. Janik, C. H. Lake, L. M. Toomey, M. R. Churchill, J. D. Atwood, *Organometallics* **1994**, *13*, 5080.
[34] M. A. Esteruelas, A. M. López, L. A. Oro, A. Péres, M. Schulz, H. Werner, *Organometallics* **1993**, *12*, 1823.
[35] A. G. Orpen, L. Brammer, F. H. Allen, O. Kennard, D. G. Watson, R. Taylor, *J. Chem. Soc. Dalton Trans.* **1989**, *S1*-S19.
[36] R. Dorta, A. Togni, R. Kissner, D. Broggini, unpublished results.
[37] R. Dorta, A. Togni, *Helv. Chim. Acta* **2000**, *83*, 119.

Received: June 10, 2003
Revised: September 16, 2003 [F5218]